DEUTSCHES ELEKTRONEN-SYNCHROTRON DESY

DESY 87-152
November 1987

受入
88-2-819
高工研図書室

TOPOLOGICAL ASPECTS OF LATTICE GAUGE THEORIES

by

A.S. Kronfeld

Deutsches Elektronen-Synchrotron DESY, Hamburg

ISSN 0418-9833

NOTKESTRASSE 85 · 2 HAMBURG 52

DESY behält sich alle Rechte für den Fall der Schutzrechtserteilung und für die wirtschaftliche Verwertung der in diesem Bericht enthaltenen Informationen vor.

DESY reserves all rights for commercial use of information included in this report, especially in case of filing application for or grant of patents.

To be sure that your preprints are promptly included in the
HIGH ENERGY PHYSICS INDEX ,
send them to the following address (if possible by air mail) :

DESY
Bibliothek
Notkestrasse 85
2 Hamburg 52
Germany

DESY 87-152
November 1987

ISSN 0418-9833

TOPOLOGICAL ASPECTS OF LATTICE GAUGE THEORIES

Andreas S. Kronfeld
Deutsches Elektronen-Synchrotron DESY, Notkestraße 85, D-2000 Hamburg 52, F.R. Germany

This review discusses topological aspects of nonabelian gauge theories defined on the lattice. The pertinent topological object is the principal bundle, so, following Lüscher, it is shown how to reconstruct the bundle from the data of the lattice gauge field. This culminates in the algorithm of Phillips and Stone for computing the topological charge, or second Chern number, of an $SU(N)$ lattice gauge field. For $SU(2)$ this algorithm is very fast. The relation of the topological susceptibility χ_t to the bare (i.e. Monte Carlo) susceptibility at nonzero lattice spacing is clarified. (The details of this discussion have a somewhat different tone than at the conference, but the conclusions are the same.) Other methods for computing the topological charge of a lattice gauge field are summarized, and the strengths and weaknesses are compared to the fiber bundle method. The numerical results of moderate to high statistics Monte Carlo determinations of χ_t are presented with remarks on scaling behavior. The review concludes with some comments on the progress, some hints of what can be done next, and some vague hope of a hidden utility for the topology of lattice gauge fields.

1. INTRODUCTION

Lattice gauge theory has two classic motivations. One is the desire to perform calculations that transcend perturbation theory and the semiclassical approximation; one would like to obtain a nonperturbative handle on hadron masses, phase structure, and, more generally, the dynamics.[1] The other motivation is the rigorous definition of the vacuum functional of generic quantum field theories, which is the continuum limit of the lattice theory.[2] Under ideal circumstances, the two perspectives will complement each other. (Semi-) rigorous developments pose precise problems which can then be attacked by brute force methods such as strong coupling expansions or numerical simulations. Conversely, the occasionally peculiar results of numerical simulations can stimulate the reformulation of the physical problem. If we are lucky, the exchange leads to a better understanding of the physics.

The topological structure of $SU(N)$ gauge fields is quantitatively summarized by the *topological susceptibility* χ_t, and the methods devised to compute it nonperturbatively in lattice gauge theory provide an example of the symbiosis between simulation and mathematics. The initial attempts[3,4] to compute χ_t faced well recognized technical and conceptual roadblocks, which together prevented a satisfactory understanding of the problem. This spurred the resolution of the conceptual part of the problem,[5] which unfortunately increased the technical barriers. More recent work has refined the conceptual framework,[6,7,8,9] so that meaningful simulations are now technically feasible; indeed the calculations for the gauge group $SU(2)$ are now very precise.[10,11] Hence, the time is right not only to review the formal developments, but also to examine the numerical work in some detail.

This Introduction ends with a lightning review of the topology of continuum gauge fields. Section 2 summarizes the physics motivations for studying gauge field topology, visiting the famous Atiyah-Singer index theorem[12] and the infamous $U_A(1)$ problem.[13] To really understand topology one must confront the theory of fiber bundles, which is done rather informally in sec. 3. Section 3 also illustrates how to reconstruct continuum topology from a lattice field using a simple toy bundle. Three available reconstructions[5,7,8,14] of the bundle of interest, the *coordinate bundle* of the gauge field, are discussed in sec. 4. Section 5 explains in detail how one extracts the susceptibility from the bare numerical calculation. Section 6 covers alternative methods for determining the topological charge of lat-

tice gauge fields and discusses their strengths and weaknesses. Numerical results for the gauge groups $SU(2)$ (refs. 10, 11, 15, and 16) and $SU(3)$ (refs. 17, 18, and 19) appear in sec. 7. Finally, sec. 8 concludes the review with miscellaneous comments and a crazy suggestion.

1.1. Topology of continuum gauge fields

Although it is inappropriate to provide a detailed review the topology of continuum gauge fields in the proceedings of a conference on lattice gauge theory, some discussion is needed to orient the rest of the review.

Formally the quantum theory of nonabelian gauge fields is defined by the vacuum generating functional

$$Z[J_\mu] = \int [dA_\mu] \exp\{-S[A_\mu] + \int d^4x \; J_\mu A_\mu\} \quad (1.1)$$

based on the classical action

$$S = \frac{1}{g^2} \int d^4x \; \mathrm{tr}\{F_{\mu\nu} F_{\mu\nu}\}, \quad (1.2)$$

$$F_{\mu\nu} = \partial_\mu A_\nu - \partial_\nu A_\mu + [A_\mu, A_\nu]$$

of the antihermitean gauge potential A_μ. Finite action (and hence nonzero Boltzmann factor) gauge fields are asymptotically pure gauge:

$$A_\mu(x \to \infty) \longrightarrow g(x) \partial_\mu g^{-1}(x). \quad (1.3)$$

The topology of g — a map from the sphere at ∞, S^3_∞, into $SU(N)$ — provides a classification of the gauge fields by the topological charge

$$Q = \frac{1}{24\pi^2} \int_{S^3_\infty} d^3x_\mu \varepsilon_{\mu\nu\rho\sigma} \mathrm{tr}\{b_\nu b_\rho b_\sigma\}$$

$$\in \Pi_3(SU(N)) = \mathbb{Z}, \quad (1.4)$$

where $b_\mu = g^{-1} \partial_\mu g$. For example, the map

$$g_1 = (x_4 + i\vec{\sigma} \cdot \vec{x})/r, \quad (1.5)$$

where $r^2 = x_4^2 + \vec{x}^2$, has $Q = 1$, and g_1^n has $Q = n$.

Another, especially cherished, expression for the topological charge is

$$Q = -\frac{1}{16\pi^2} \int d^4x \; \mathrm{tr}\{F_{\mu\nu} {}^*F_{\mu\nu}\}, \quad (1.6)$$

$${}^*F_{\mu\nu} = \frac{1}{2} \varepsilon_{\mu\nu\rho\sigma} F_{\rho\sigma}.$$

Section 3 contains a proof that eq. (1.4) and eq. (1.6), appropriately interpreted, are identical. From eq. (1.2), eq. (1.6), and the inequality

$$\int d^4x \; \mathrm{tr}\{(F_{\mu\nu} \pm {}^*F_{\mu\nu})^2\} \geq 0, \quad (1.7)$$

one sees that the action in a given Q-sector is bounded by

$$S \geq |Q| \frac{8\pi^2}{g^2}. \quad (1.8)$$

The inequality is saturated by solutions of the (Euclidean) equations of motion, called *instantons*, which are (anti-) selfdual,[20] i.e. $F_{\mu\nu} = \pm {}^*F_{\mu\nu}$. For example, the one instanton solution has a gauge potential

$$A_\mu = \frac{r^2}{r^2 + \rho^2} g_1^{-1} \partial_\mu g_1 \quad (1.9)$$

where the size ρ of the instanton is an arbitrary scale.

Now consider the classical vacuum state $|0\rangle$ characterized by $A_\mu = 0$ — up to gauge transformations. Gauss' law requires that $|0\rangle$ be invariant under infinitesimal gauge transformations, but it says nothing about homotopically nontrivial transformations such as g_1. Hence, there is an infinite sequence of classical vacua

$$|n\rangle \equiv T_1^n |0\rangle, \quad (1.10)$$

where T_1 is the unitary operator implementing the gauge transformation g_1, and n is any integer. Due to tunnelling caused by the instantons, the quantum vacuum is described by a superposition of the $|n\rangle$, and since T_1 commutes with the Hamiltonian, one finds[21]

$$|\theta\rangle = \sum_n e^{i\theta n} |n\rangle. \quad (1.11)$$

The vacuum parameter θ is a new and unexpected feature of QCD. If it is nonzero, the path integral, eq. (1.1), is modified by the substitution $S \to S + i\theta Q$, and then CP is violated. In our world θ is exceedingly tiny, and it is quite possible that it is tuned to zero by a non-QCD mechanism.[22]

The topological structure sketched above is in marked contrast to QED, where the gauge function is

Table 1: Squared masses of the light pseudoscalar and vector mesons in units of the proton mass.

0^{-+} meson	m^2	1^{--} meson	m^2
π	0.02	ρ	0.67
K	0.28	K^*	0.90
η	0.34	ω	0.70
η'	1.04	ϕ	1.18

always homotopic to the identity. This observation has inspired the idea that the topological structure is "responsible" for the contrasting properties of abelian and nonabelian gauge theories. Neglecting subtleties, instantons augment the usual perturbative series:

$$\begin{aligned}\langle \mathcal{O} \rangle = \; & C_0(1 + a_0^{(2)} g^2 + \cdots) \\ + \; & C_1 e^{-8\pi^2/g^2}(1 + a_1^{(2)} g^2 + \cdots) \\ + \; & C_2 e^{-2(8\pi^2/g^2)}(1 + a_2^{(2)} g^2 + \cdots) + \cdots,\end{aligned} \tag{1.12}$$

but because of the $\exp(-S) = \exp(-8\pi^2/g^2)$ behavior, the instantons' contribution is usually small when semiclassical and perturbative techniques are applicable. If topologically nontrivial configurations play an important role, then only at scales where the effective coupling is large, and then one has a truly nonperturbative problem. This in turn implies that we are obliged to formulate and understand the topology of gauge fields using the lattice as the regulator.

2. PHYSICAL MOTIVATION

Before discussing the formulation of the topology of lattice gauge fields and its implementation in numerical simulations, it is useful to recall the physical motivation. Here I will summarize the $U_A(1)$ problem and the Atiyah-Singer index theorem, because they indicate the role that topology can play in understanding the hadron masses, and there is very little that is more physical than masses. Table 1 contains the masses of the pseudoscalar and vector meson nonets, in units of the proton mass.

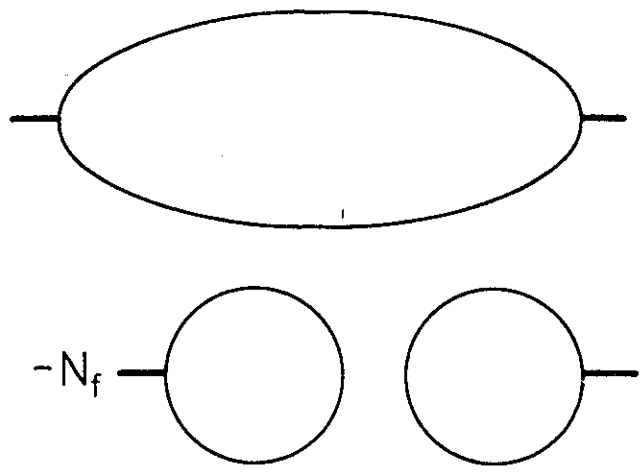

Figure 1: Diagrammatic representation of the flavor singlet meson propagator in terms of quark propagators. (Gluon contributions are implicitly included.)

2.1. The $U_A(1)$ problem

The pattern in the vector sector is easy to understand using the quark model with a strange quark rather heavier than the up and down quarks. The small masses of π and K, on the other hand, can be understood through the Goldstone phenomenon. However, the magnitude of the η and η' masses is less clear. Ultimately, the π-η-η' splitting is due to the extra diagram depicted in fig. 1, so the real mystery[23] is that $m_\eta^2 - m_\pi^2 \gg m_\omega^2 - m_\rho^2$. The most precise formulation of the problem is Weinberg's bound,[13] based on $U(N_f) \times U(N_f)$ current algebra, with $N_f = 3$. To leading order in m_π^2/m_K^2 the $I_3 = 0$ pseudoscalar (π^0, η, η') mass matrix has eigenvalues m_π^2, $3m_\pi^2/(1+2z^2)$, and $4m_K^2(1+2z^2)/6z^2$, where $z = f_{\eta'}/f_\pi$. The first mass obviously corresponds to the pion, but it is impossible to reconcile the η and η' masses with the other two expressions. In particular, there is no particle with $m^2 < 3m_\pi^2$ as implied by the second eigenvalue.

The motivation for $U(N_f) \times U(N_f)$ is QCD, whose classical Lagrangian is invariant under that chiral symmetry group in the massless limit. Of course, the classical Lagrangian is not the full story, and to define the

quantum theory one must regulate the vacuum functional. The regulator inevitably breaks the $U_A(1)$ component of the chiral symmetry. Specifically, the $U_A(1)$ Noether current

$$J^5_\mu = \sum_{f=1}^{N_f} \bar{\psi}_f \gamma_\mu \gamma_5 \psi_f \tag{2.1}$$

is broken by the Adler-Bell-Jackiw anomaly:[24]

$$\partial_\mu J^5_\mu = -2N_f q, \quad q = -\frac{1}{16\pi^2}\mathrm{tr}\{F_{\mu\nu}{}^*F_{\mu\nu}\}, \tag{2.2}$$

If $\mathrm{tr}\{F_{\mu\nu}{}^*F_{\mu\nu}\}$ were "zero," the anomaly explanation of the $U_A(1)$ problem would be inadequate. However, the integral of the Chern-Pontryagin density q

$$\int d^4x\, q = Q \in \mathbb{Z} \tag{2.3}$$

is exactly the topological charge as in eq. (1.6). The anomaly hence provides an *explicit* breakdown of the $U_A(1)$ symmetry, so that $SU(N_f) \times SU(N_f)$ is the correct current algebra, and the bound $m^2 < 3m_\pi^2$ no longer applies.

The topological resolution of the $U_A(1)$ problem is made quantitative by the *Witten-Veneziano formula*, which relates the "topological susceptibility" in a spacetime volume V

$$\chi_t \equiv \int d^4x\, \langle q(x)q(0)\rangle = \frac{\langle Q^2\rangle}{V} \tag{2.4}$$

to the pseudoscalar masses. In the large N_c limit one can derive[25]

$$\chi_t^{\text{quenched}} = \frac{f_{\eta'}^2 m_{\eta'}^2}{2N_f} \tag{2.5}$$

$$= \frac{f_\pi^2}{2N_f}(m_{\eta'}^2 + m_\eta^2 - 2m_K^2) = (180\mathrm{MeV})^4.$$

The second equality in eq. (2.5) is a refinement in two regards. Firstly, the experimentally unknown decay constant $f_{\eta'}$ has been replaced with the pion decay constant f_π (which is consistent in the large N_c expansion), and secondly the effects of small nonzero quark masses has been taken into account. The quenched approximation arises because the effects of quark loops are suppressed at large N_c. Indeed, in the same scenario one finds

$$\chi_t^{\text{full QCD}} = \frac{f_\pi^2 m_\pi^2}{2N_f}, \tag{2.6}$$

which is consistent with the observation that observables must be independent of θ in the chiral limit.[26,21]

The Witten-Veneziano formula has become a Holy Grail to those involved in numerical simulation. The interesting susceptibility is in the pure glue theory, for which the Monte Carlo problem is drastically simpler than for full QCD. (To compare the two, see elsewhere in the Proceedings.) However, it is easy to get too carried away with the value of 180 MeV. Remember, it is based on the large N_c equivalence of the decay constants and genuine $N_c = 3$ masses, and it will be compared either to a very precise susceptibility computation for $N_c = 2$, or to a *low statistics* computation for $N_c = 3$. 180 MeV is really only a guide.

2.2. Atiyah-Singer index theorem

At the semiclassical level the interplay between the topology of the gauge field and the breakdown of chiral symmetry in made explicit by the Atiyah-Singer index theorem. In the continuum the Dirac operator satisfies[12]

$$\mathrm{ind}(\not{D}) = Q, \quad \not{D} = \not{\partial} + \not{A} \tag{2.7}$$

where the Atiyah-Singer index

$$\mathrm{ind}(\not{D}) = \lim_{m\to 0} \mathrm{Tr}\left(\gamma_5 \frac{m}{\not{D} + m}\right) = n_+ - n_- \tag{2.8}$$

is the difference between the number of $+$ and $-$ (n_+ and n_-) chirality zero modes of $\not{D}$. Here Tr denotes the "trace" over spacetime indices as well as internal ones.

For example, in an instanton configuration one finds[26] that the quark field ψ has a zero mode ($\not{D}\psi = 0$), but the conjugate field $\bar{\psi}$ does not ($\bar{\psi}\not{D} \neq 0$). Then the simple rules of Berezin integration show that the chiral condensate $\langle\bar{\psi}\psi\rangle \neq 0$. This underscores the way in which topologically nontrivial configurations, through the anomaly, explicitly break the $U_A(1)$ symmetry and

generate a mass for the η'. Furthermore, if one studies quark-instanton interactions at small mass in the semi-classical approximation,[27] one finds that as $m_q \to 0$ the theory enters the phase with spontaneously broken chiral symmetry. Thus, topology can account for the small π and K masses in Table 1, too.

It is worth emphasizing that the index theorem is a relation between the continuum Dirac operator and a continuum (i.e. sufficiently smooth) gauge field. To the best of my knowledge there is no known lattice approximant to the Dirac operator with the topological properties necessary to fulfill the index theorem. Consequently, much of what one assumes about the dynamics of QCD will appear in simulations with dynamical quarks only at exceedingly small lattice spacing. Only then will $\det(\not{D} + m)$ adequately reproduce the implications of the index theorem.

Recently Smit and Vink have rederived the Witten-Veneziano formula in a very straightforward way using Ward-Takahashi identities.[28] Their derivation uses the lattice regulator, so it is also valid on a formal level in the continuum. However, the direct approach yields eq. (2.5) but with the susceptibility of the Atiyah-Singer index on the left-hand-side. In the continuum the two susceptibilities are equal, but with either Wilson or staggered fermions they are not. Moreover, there are a variety of details which make a numerical computation of $\mathrm{ind}(\not{D})$ problematic. This is sketched in sec. 6, below, and elaborated in Vink's contribution to this conference.[29]

3. FIBER BUNDLES

To incorporate topological considerations into lattice gauge theory, one must keep the appropriate mathematical framework in mind, and that is the framework of fiber bundles. Most physicists know what a fiber bundle is, even if the mathematicians' language sounds foreign. The most expeditous way of establishing a common ground is to provide a dictionary (Table 2) and a few examples. Physicists who wish a more thorough

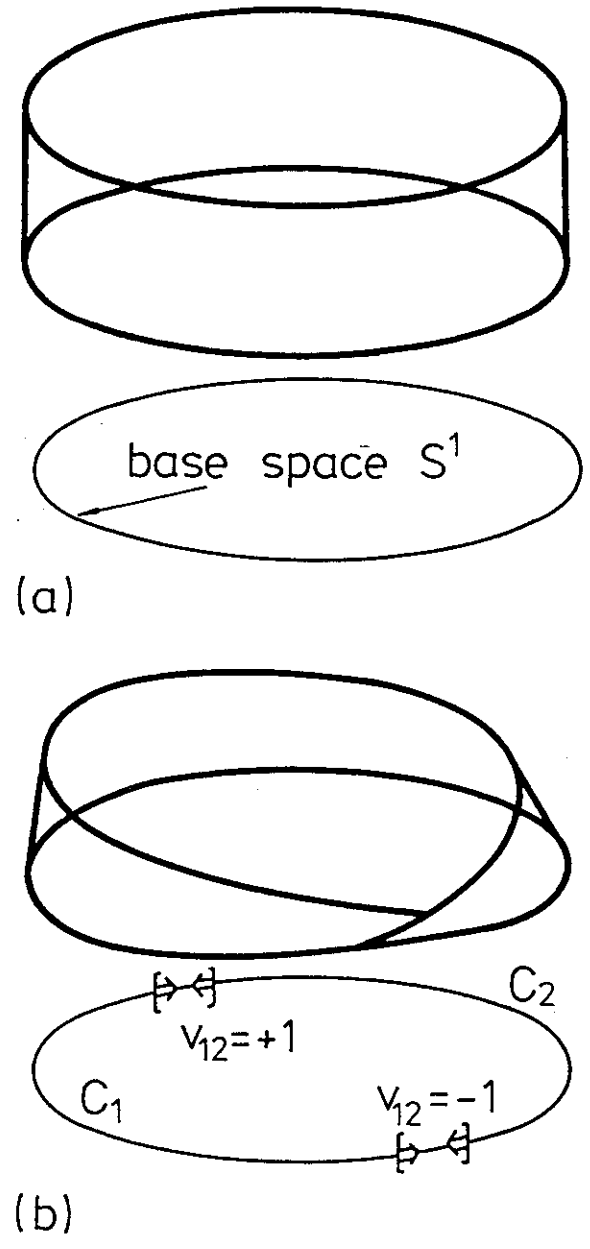

Figure 2: Two fiber bundles over S^1. The simple strip (a) is trivial, whereas the Möbius strip (b) is not.

Table 2: Relation between mathematicians' language of fiber bundles and physicists' language of field theory.

mathematicians' language	**physicists' language**
base space M	spacetime
open cover, $\{c_\alpha\}$	a set of cells in spacetime
fiber F	set of possible values of $\phi(x)$
total space P	set of all *topologically distinct* fields
projection $\pi : P \to M$ and its inverse $\pi^{-1} : M \to P$	associates a fiber to $x \in M$
stucture group G	gauge group
transition functions, $v_{\alpha\beta}$	gauge transformation from c_α to c_β
associated fiber bundle: $F = V$	matter fields in vector space V
principal fiber bundle: $F = G$	gauge fields with group G
connection ω	gauge potential A_μ

exposition of the concepts should consult the very nice article by Daniel and Viallet.[30]

Over a cell in the open cover the bundle is a product of the base space and the fiber: in equations $\pi^{-1}(c_\alpha) = c_\alpha \times F$. However, for a nontrivial bundle the local product structure cannot be extended globally. An instructive example is a simple strip and the Möbius strip, depicted in fig. 2. The base space is the circle S^1, the fiber is the unit interval $[0,1]$, and the structure group is $\mathbb{Z}_2$, corresponding to the identity and a flip about the midpoint of the fiber. The simple strip, fig. 2a is trivial; in the open cover only one cell is necessary, or equivalently, all transition functions may be taken to be unity. On the other hand, the Möbius strip, fig. 2b, has a nontrivial twist; the open cover requires at least two cells, and on one of the overlaps the transition function cannot be unity.

For the incorporation of the bundle idea into a lattice field theory, the associated bundles depicted in fig. 3 are illuminating. Again the structure group is $\mathbb{Z}_2$, but now the fiber is the oriented real line, or "ray." Fig. 3a is trivial and fig. 3b is not. For artistic reasons the fibers have been drawn to emanate from the base space S^1, and not all of them have been drawn. But one can just as easily interpret fig. 3 as depicting lattice fields. The eye naturally interpolates fig. 3b into a nontrivial bundle, yet it leaves fig. 3a trivial. Keeping fig. 3 in

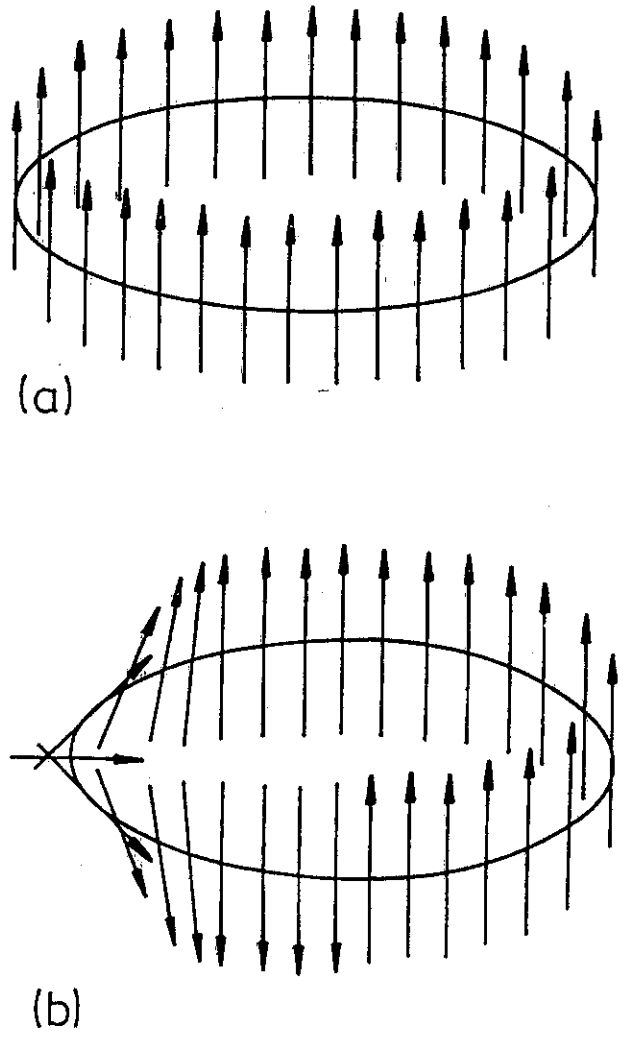

Figure 3: Two associated fiber bundles over S^1. (a) is trivial, whereas (b) is not.

mind, let us consider the naive topological notion of "continuous deformation." By changing the fiber over each lattice site individually, one can imagine deforming the nontrivial bundle into the trivial one. If one wishes to define a field theory where topological nontrivial configurations play an important dynamical role, then this notion of continuous deformation must be discarded and replaced with a more restrictive notion. A sufficient constraint is a bound on an "action density:" $s \equiv 1 - \cos(2\theta_{i,i+1}) < \delta$, for some appropriately chosen δ, where $\theta_{i,i+1}$ is the angle between neighboring rays. Then, if one forbids deformations that produce $s \geq \delta$, the topological distinction between figs. 3a and 3b remains.

The reconstruction of the associated bundle can be taken further. Let φ and θ denote the angular coordinate of S^1 and the angular orientation of the rays, respectively; let subscripts $i, j, \ldots$ refer to lattice sites; and let c_i be the dual cell surrounding lattice site i. The $\{c_i\}$ is the open cover. Next introduce the proviso that $|\theta_i - \theta_{i+1}| > \pi/2$ implies a twist, i.e. the transition function $v_{i,i+1} \in \mathbb{Z}_2$ is -1. Then, interpolation linear in φ from $\sin(\theta_i)$ to $\sin(v_{i,i+1}\theta_{i+1})$, as φ ranges from φ_i to φ_{i+1}, provides a continuum field with the right topological properties. Finally, if an ensemble of configurations is produced under some dynamics that enforce the smoothness constraint, then one can construct a quantum field theory where topology makes sense.

To give a meaning to the topology of lattice gauge fields, one must devise a similar, albeit more sophisticated, interpolation. As in the example, the unique reconstruction of a principle fiber bundle from the lattice gauge field requires a bound on the action density. However, such a restriction is not devastating for nonabelian gauge theory, because the dynamics are asymptotically free, and the fields do indeed become smoother in the continuum limit.

4. BUNDLE RECONSTRUCTION

In nonabelian gauge theory the practical goal (χ_t in quenched QCD) and the abstract ideas outlined above lead one to reconstruct the principal bundle from the data of the lattice gauge field. Reconstructing the *coordinate bundle*, that is the set of transition functions, is entirely satisfactory, because the topological charge is the second Chern number of the coordinate bundle.

Consider the $\mathrm{tr}\{F_{\mu\nu}{}^*F_{\mu\nu}\}$ expression for the topological charge.

$$Q = \int d^4x\, q = -\frac{1}{16\pi^2}\int d^4x\, \mathrm{tr}\{F_{\mu\nu}{}^*F_{\mu\nu}\}, \quad (4.1)$$

An immediate problem is that most lattice approximants to q have no topological significance. For example,[4,31,32]

$$q_{\mathrm{naive}} \sim \varepsilon_{\mu\nu\rho\sigma}\mathrm{tr}\{U_{\mu\nu}U_{\rho\sigma}\} \quad (4.2)$$

has $O(a^2)$ corrections multiplying ultraviolet divergent operators, which yield nontopological contributions of $O(a^0)$. Consequently, $\int d^4x\, q_{\mathrm{naive}} \notin \mathbb{Z}$. One *can* devise lattice approximants to the Chern-Pontryagin density, but they are impossible to guess; to derive them one must do some topology.

Thus, consider the spacetime manifold M and write[33]

$$\mathrm{M} = \mathbb{T}^4 = \bigcup_\alpha c_\alpha; \quad (4.3)$$

the 4-torus is convenient because of the eventual lattice simulations, but all that matters for the derivation is $\partial\mathrm{M} = 0$. The cells c_α consitute the open cover, and on the lattice they are, e.g. hypercubes or 4-simplices. In each cell pick a smooth gauge

$$A_\mu^{(\alpha)} = g_\alpha(\partial_\mu + A_\mu)g_\alpha^{-1}, \ \text{on}\ c_\alpha. \quad (4.4)$$

The g_α are called local sections; a bundle is nontrivial if it is impossible to extend the section to all $x \in \mathrm{M}$. On the overlaps $c_{\alpha\beta} \equiv c_\alpha \cap c_\beta$ the gauge potentials are related by

$$A_\mu^{(\alpha)} = v_{\alpha\beta}(\partial_\mu + A_\mu^{(\beta)})v_{\beta\alpha}. \quad (4.5)$$

The *transition functions*

$$v_{\alpha\beta} = g_\alpha g_\beta^{-1} = v_{\beta\alpha}^{-1} \tag{4.6}$$

describe how the gauge field is patched together. For consistency the transition functions must satisfy

$$v_{\alpha\gamma} = v_{\alpha\beta} v_{\beta\gamma} \tag{4.7}$$

on double overlaps $c_{\alpha\beta\gamma} = c_\alpha \cap c_\beta \cap c_\gamma$. Equation (4.7) is called the cocycle condition.

Mathematicians often consider arbitrary overlaps. For our purposes, it is useful to arrange the cells so that they are "just touching," i.e. so that $\dim c_{\alpha\beta} = 3$ and $\dim c_{\alpha\beta\gamma} = 2$, etc.

Topology concerns overall characteristics of the fields, not details like the value of $F_{\mu\nu}(x)$ in volts per meter. Hence, if Q warrants the name "topological charge," one ought to seek an expression for Q in terms of the $v_{\alpha\beta}$. To achieve this write

$$\begin{aligned} Q &= -\frac{1}{16\pi^2} \sum_\alpha \int_{c_\alpha} d^4x \ \mathrm{tr}\{F_{\mu\nu}^{(\alpha)*} F_{\mu\nu}^{(\alpha)}\} \\ &= \sum_\alpha \int_{c_\alpha} d^4x \ q^{(\alpha)}. \end{aligned} \tag{4.8}$$

The Chern-Pontryagin density $q^{(\alpha)}$ is a total derivative: $q^{(\alpha)} = \partial_\mu \Omega_\mu^{(\alpha)}$, where

$$\Omega_\mu^{(\alpha)} = -\frac{1}{8\pi^2} \varepsilon_{\mu\nu\rho\sigma} \mathrm{tr}\{A_\nu^{(\alpha)} (\partial_\rho A_\sigma^{(\alpha)} + \frac{2}{3} A_\rho^{(\alpha)} A_\sigma^{(\alpha)})\} \tag{4.9}$$

is the Chern-Simons form. By construction $\Omega_\mu^{(\alpha)}$ is once differentiable, so one can integrate the expression for the charge and obtain

$$Q = \sum_\alpha \int_{\partial c_\alpha} d^3x \, {}_\mu \Omega_\mu^{(\alpha)} = \frac{1}{2!} \sum_{\alpha,\beta} \int_{c_{\alpha\beta}} d^3x \, {}_\mu (\Omega_\mu^{(\alpha)} - \Omega_\mu^{(\beta)}) \tag{4.10}$$

Using eq. (4.5) on $\Delta\Omega_\mu^{(\alpha,\beta)} = \Omega_\mu^{(\alpha)} - \Omega_\mu^{(\beta)}$ allows one to eliminate the gauge potentials. The result, first derived independently by Lüscher[5] and by van Baal,[34] is

$$Q = +\frac{1}{8\pi^2} \sum_{\alpha<\beta<\gamma} \int_{c_{\alpha\beta\gamma}} d^2x_{\mu\nu} \varepsilon_{\mu\nu\rho\sigma} \mathrm{tr}\{a_\rho^{(\gamma,\beta)} a_\sigma^{(\alpha,\beta)}\} \tag{4.11}$$

$$-\frac{1}{24\pi^2} \sum_{\alpha<\beta} \int_{c_{\alpha\beta}} d^3x_\mu \varepsilon_{\mu\nu\rho\sigma} \mathrm{tr}\{a_\nu^{(\alpha,\beta)} a_\rho^{(\alpha,\beta)} a_\sigma^{(\alpha,\beta)}\},$$

where $a_\mu^{(\alpha,\beta)} = v_{\beta\alpha} \partial_\mu v_{\alpha\beta}$. Equation (4.11) verifies the claim that the topological charge is an invariant of the coordinate bundle.

For numerical work there is a even nicer formula, obtained by eliminating the $v_{\alpha\beta}$ in terms of the g_α:

$$Q = \sum_\alpha Q_\alpha.$$

In this expression each term is an integer:

$$Q_\alpha = -\frac{1}{24\pi^2} \int_{\partial c_\alpha} d^3x_\mu \varepsilon_{\mu\nu\rho\sigma} \mathrm{tr}\{b_\nu^{(\alpha)} b_\rho^{(\alpha)} b_\sigma^{(\alpha)}\}, \tag{4.12}$$

where $b_\mu^{(\alpha)} = g_\alpha^{-1} \partial_\mu g_\alpha$. Mathematicians call the sum of the Q_α the second Chern number. Equation (4.12) is in fact eq. (1.4). The finite action condition imposes a boundary condition, so that spacetime acquires the topology of a sphere: M = S^4. The two cells are the interior and exterior of a ball surrounding the point at ∞; in the interior of the ball the section is g_1, eq. (1.5), and in the exterior the section is trivial.

4.1. Explicit construction of the $v_{\alpha\beta}$

The task ahead is to define transition functions or local sections using the lattice gauge field as input. One wants the interpolations to be as smooth as possible on scales smaller than the lattice spacing. The transition functions must obey the cocycle condition, and the associated expression for the Chern-Pontryagin density must have the right classical continuum limit.

There are three bundle reconstruction algorithms on the market, by Lüscher,[5] by Woit,[7] and by Phillips and Stone.[8] Each one picks a convenient shape cell, and a convenient gauge in each cell. Then the local sections or the transition functions are given at certain points on the lattice. From those points the transition functions are reconstructed by interpolating along geodesics in the gauge group, first in one dimension, then two, ... All fail to give a well-defined charge for a set of configurations of measure zero in the path integral; these configurations, referred to as *exceptional configurations*, form the boundaries of the topological

sectors. They arise when certain group geodesics in the interpolation become ill-defined.

Lüscher[5] takes the hypercubes in a hypercubic lattice as his cells, and fixes to complete axial gauge in each cell. The gauge function g_α is then a product of link matrices on a path back to the "origin" of the hypercube. For a given site the gauge function is generally different for each hypercube to which the site belongs, and the product $g_\alpha g_\beta^{-1} = v_{\alpha\beta}$ yields the transition functions at each site in the lattice. Using interpolation functions of increasing complexity Lüscher then gives expressions for the transition functions on links, plaquettes, and cubes. Unfortunately ref. 5 does not give explicit expressions for the section. However, after a long bout of head-scratching, pencil-chewing, and desk-pounding, Wiese succeeded in writing down a section that returns Lüscher's transition funcitions.[14,19]

Soon after Lüscher's work Woit[6] recognized that viable computations would only be feasible using eq. (4.12), and he provided an algorithm that goes straight for the local sections.[35] Woit's (modified and improved) algorithm[7] takes timeslices to be the cells, and fixes to $A_0^{(t)} = 0$, $\vec{\nabla} \cdot \vec{A}^{(t)} = 0$ gauge. (N.B. $A_0 = 0$ is not possible globally on a torus.) At a given lattice site the section is trivial in the preceding timeslice, and given by the timelike link in the subsequent timeslice. The section is then defined throughout the rest of the timeslice by interpolating the timelike links along geodesics. For this purpose $A_0^{(t)} = 0$ gauge is sufficient; the point of the Coulomb gauge fixing, is that the interpolation becomes smoother, and smoothness simplifies the numerical evaluation of the Q_α.

The most appealing algorithm is that of Phillips and Stone.[8] For $SU(2)$ it has the special virtue that it is *fast*. For geometric reasons Phillips and Stone work on a simplicial lattice, and their cells are intersections of the 4-simplices and the dual cells. In each dual cell c_α, surrounding the lattice site $x^{(\alpha)}$, they fix to radial gauge, $A_\mu^{(\alpha)}(x - x^{(\alpha)})_\mu = 0$. This gauge condition means that there is trivial parallel transport along radial paths *within* a dual cell. Consequently, to preserve the (gauge covariant) parallel transport $u_{\alpha\beta}$ along the link from $x^{(\alpha)}$ to $x^{(\beta)}$ one must have

$$v_{\alpha\beta}(x^{(\alpha,\beta)}) = u_{\alpha\beta}, \tag{4.13}$$

where $x^{(\alpha,\beta)}$ is the midpoint of the link from $x^{(\alpha)}$ to $x^{(\beta)}$. With the transition functions fixed at the $x^{(\alpha,\beta)}$, we must now consider the interpolation. Phillips and Stone do so within each $c_\alpha^\sigma = \sigma \cap c_\alpha$, where σ is a simplex with $x^{(\alpha)}$ as a vertex. Given an ordering of the vertices in σ, the interpolation proceeds as follows:

- if $\beta = \alpha \pm 1$ (in the ordering of σ), then $v_{\alpha\beta}$ remains constant on $c_{\alpha\beta}^\sigma$.
- if $\beta = \alpha \pm 2$, then let γ be the intervening vertex, and note that there are two constraints: the value $u_{\alpha\beta}$ at the midpoint and the cocycle condition on $c_{\alpha\gamma\beta}^\sigma$. In the direction $\vec{\gamma}$ towards γ the transition function varies geodesically $v_{\alpha\beta} = u_{\alpha\beta}(u_{\beta\alpha}u_{\alpha\gamma}u_{\gamma\beta})^{z_\gamma}$, where z_γ is a coordinate labelling the line segment from the midpoint $x^{(\alpha,\beta)}$ to the medial point of $\tau \subset \sigma$, the triangle defined by the vertices $\alpha\gamma\beta$. In the directions orthogonal to $\vec{\gamma}$ the transition function stays constant.
- if $\beta = \alpha \pm n$, then the transition function is interpolated in the $n-1$ directions labelled by the $n-1$ intervening vertices, and it remains constant in the others. For explicit formulae, consult ref. F.

The strategy is inductive: the interpolation across an n-dimensional simplex builds on the interpolation across the $(n-1)$-dimensional subsimplices.

This construction may seem rather baroque, but the explanation of the algorithm is more confusing than the geometry of the transition functions.[36] As with good baroque art, careful scrutiny is needed to appreciate the beauty of the bundle. For a simplicial lattice Phillips' and Stone's transition functions are "as close as possible" to the lattice gauge field, i.e. the geodesic distance $d(v_{\alpha\beta}, u_{\alpha\beta})$ is minimal. Indeed, from the above

description the reader can see that often $v_{\alpha\beta} = u_{\alpha\beta}$. The as-close-as-possible principle allows one to prove various theorems about the uniqueness of the reconstructed bundle. All of the theorems have hypotheses of the form

$$d(1, u_P) \leq \delta, \tag{4.14}$$

where and u_P represents parallel transport around an arbitrary loop in a simplex. In particular, for $\delta = \pi/2$ the bundle is independent of the ordering, and for $\delta = \pi/8$ the bundle is unique, in the sense that *all* transition functions satisfying eq. (4.14) with $\delta = \pi/8$ yield the same topological charge.

The inductive nature of their scheme enables them to obtain a set of local sections corresponding to their transition functions by a neat trick. By adding one site in a fifth dimension, connected to every site in the original lattice by a link with trivial parallel transport, one constructs a cone with the 4-dimensional lattice as its base. Then, lo and behold, the transition functions of the 5-dimensional lattice, constructed by Phillips' and Stone's algorithm, yield a section of the 4-dimensional bundle!

4.2. Computing the Q_α

Except for ref. 37, which used eq. (4.11) at a time when only Lüscher's transition functions were available, all applications of fiber bundle methods for computing the topological charge have used eq. (4.12). For $SU(2)$ the task is to evaluate the Q_α, the *winding number* of the local sections g_α. This can be done geometrically. Pick an arbitrary probe $y \in SU(2)$, and let x_i denote points on ∂c_α such that $g_\alpha(x_i) = y$. Then the winding number is given by

$$Q_\alpha = \sum_i \operatorname{sign} \left\| \left. \frac{\partial g_\alpha}{\partial x} \right|_{x_i} \right\|. \tag{4.15}$$

The summand is the orientation of the map g_α at x_i. The strategy is then to break g_α into spherical polyhedra with geodesic edges. Then for arbitrary y one can determine the existence and number of x_i, and the orientation of g_α at x_i using combinatoric formulae. In contrast the integrals in eq. (4.11) must be integrated numerically to sufficent precision to yield an integer after the summation over all cells.[37]

Using Woit's algorithm[7] or the section[14] for Lüscher's bundle always involves explicit interpolation. Typically, the region ∂c_α is chopped in to tiny tetrahedra, each small enough so that $g_\alpha(\partial c_\alpha)$ can be approximated by a spherical tetrahedron. Then the location of the probe can be determined using 4×4 determinants. The beauty of the Phillips and Stone algorithm is that the structure of the section is such that it defines large *exact* spherical polyhedra. It is then possible to evaluate the topological charge in $SU(2)$ computing only 4×4 determinants and the roots of a quadratic equation.

Unfortunately, $SU(3)$ is not so simple, even for Phillips and Stone, because the $SU(3)$ manifold is enormously more complicated geometrically. A promising idea is the reduction of the structure group from $SU(3)$ to $SU(2)$,[38,9] which can also be extended to $SU(N)$.[14] However, this can not be applied straightforwardly, because a reduced $SU(3)$ geodesic interpolation is not a $SU(2)$ geodesic interpolation. Instead, one must again chop up ∂c_α into tiny $SU(3)$ tetrahedra, for which $g_\alpha(\partial c_\alpha)$ are approximated by the $SU(2)$ geodesic tetrahedron whose corners are given by reduction. The need in $SU(3)$ for explicit interpolation is still the barrier preventing high statistics calculations.

4.3. Summary

In summary, a bundle reconstruction algorithm splits the set of all lattice gauge fields into topological classes by defining transition functions based on the data of the lattice gauge field. In general this involves raising closed loops to fractional powers, which is not always well-defined, leading to exceptional configurations. These exceptional configurations form the boundary of the topological sectors: in order to continuously deform a $Q = 1$ configuration into a $Q = 0$, one must pass through an exceptional configuration. For a given configuration the charge may also depend on certain technical details of the algorithm (choice of time

axis, or ordering of the vertices). However, sufficiently smooth configurations have a unique charge;[8] the way in which sufficient smoothness is attained in asymptotically free quantum field theories is the subject of the next section.

5. CALCULATING χ_t

It is now time to turn to quantum field theory. This means the properties of the ensemble are more crucial than the individual configurations. It also means that one must worry about how the cutoffs effect the extraction of physically relevant information from a calculation. In a numerical simulation, there are two cutoffs: the volume and the lattice spacing. The finite volume effects are presumably straightforward, and discussion of them is deferred to sec. 7. (They are also not much discussed in the literature.) The nonzero lattice spacing effects are subtle, and their removal is the topic of this section.

In order to firmly anchor the discussion it is useful to introduce the θ-dependent partition function

$$Z(\theta) = \sum_Q e^{i\theta Q} \mathrm{P}_Q. \qquad (5.1)$$

The probability P_Q for a configuration to have charge Q is given (formally) by

$$\mathrm{P}_Q = \frac{\int [dA_\mu]_Q \exp\{-S[A_\mu]\}}{\int [dA_\mu] \exp\{-S[A_\mu]\}} \qquad (5.2)$$

where the path integration in the numerator is restricted to the sector with topological charge Q. The P_Q are directly determined in the numerical simulation, and furthermore they are observable quantities, because knowledge of them is equivalent to knowledge of the connected moments of Q,

$$\langle Q^n \rangle_c \equiv \left(\frac{\partial}{i\partial\theta} \right)^n \ln Z(\theta). \qquad (5.3)$$

For spacetime volume V, $\langle Q^n \rangle_c / V$ is the n-point function of the Chern-Pontryagin density $q(x)$ at zero four-momentum, and is hence related to the propagators and/or couplings of states in the $J^P = 0^-$ channel.

Even though the statement is trivial, it is important to stress that accurate and precise determination of the P_Q, eventually in the limits of infinite volume and of vanishing lattice spacing, is the fundamental objective. Recall that the charge assigned to a given configuration can depend on certain technical details in the algorithms. For instance, in the Phillips and Stone algorithm the charge can depend on the ordering of the vertices. This effect will not alter the distribution in any substantial way. Given a sufficiently large ensemble, configurations with all possible orientations with respect to the ordering will appear, so that ensemble averages, such as the P_Q, no longer have any vertex order dependence. It can happen that different algorithms yield slightly different bare distributions at finite ultraviolet cutoff, but all bare quantities have such violations of universality when the cutoff is finite.

5.1. Cutoff dependence I: usual case

For a typical matrix element the bare expression $\langle \mathcal{O} \rangle^0$ is related to the renormalized $\langle \mathcal{O} \rangle$ by

$$\langle \mathcal{O} \rangle^0 = Z_{\mathcal{O}} \kappa_{\mathcal{O}} \langle \mathcal{O} \rangle + C_{\mathcal{O}} (a\Lambda)^{p_1} |\ln(a\Lambda)|^{p_2} + \cdots, \qquad (5.4)$$

where a is the inverse ultraviolet cutoff (e.g. lattice spacing), and Λ is the renormalization group invariant mass scale. The renormalization constant $Z_{\mathcal{O}}$ is responsible for the anomalous dimension of the operator $\mathcal{O}$. Usually $Z_{\mathcal{O}} \neq 1$, and then $\kappa_{\mathcal{O}}$ can be absorbed into $Z_{\mathcal{O}}$. (One might find different $\kappa_{\mathcal{O}}$ in different regularization-renormalization schemes, but then scale changes compensate the absorption into $Z_{\mathcal{O}}$ — cf. ref. 39.) Noether currents "J" of symmetries of the theory are physical observables, so they have no anomalous dimension: $Z_J = 1$. Especially in lattice field theory, one is occasionally driven to consider an approximant to a Noether current that is no longer an exact Noether current. For example, the Noether current of global vector gauge symmetries on the lattice is $(\bar{\psi}\gamma_\mu U_\mu \psi + \mathrm{h.c.})/2$ — in a schematic notation — not the popular $\bar{\psi}\gamma_\mu\psi$. Using the latter one encounters $\kappa_J \neq 1$, and one must devise a technique of computing it, preferably nonperturba-

tive, although weak coupling perturbation theory can give a reliable guide to the structure. Finally, the C_O term represents generic nonuniversal terms. If $p_1 > 0$ one usually neglects them, because in the continuum limit $a\Lambda \ll 1$; otherwise a sensitive subtraction must be made. All of this is well known to those computing matrix elements relevant to QCD scattering[39,40,41] or to weak decays.[42,43]

5.2. Cutoff dependence II: $\langle Q^n \rangle_c$

Now let us focus on the topological susceptibility $\chi_t \equiv \langle Q^2 \rangle_c / V$, which is more complicated because everything is nonperturbative. The arguments hold for the other moments also.

In the continuum χ_t has no anomalous dimension, and since no one would consider a lattice Chern-Pontryagin density q with the incorrect naive continuum limit, we can set $Z_\chi = 1$. However, only certain choices of Q will have $\kappa_\chi = 1$. The formal proof that Noether currents have $\kappa_J = 1$ requires the equations of motion. The analagous step for the susceptibilty requires

$$\frac{\delta Q}{\delta A_\mu(x)} = 0. \qquad (5.5)$$

The topological charge based on a fiber bundle shares this property. If ∂_t denotes differentiation with respect to link matrix U_t, then $\partial_t Q = 0$, because it is piecewise constant over $\{U_t\}$.

Other approaches to the topological susceptibility do not respect eq. (5.5), however, and therefore face the difficult task of determining κ_χ nonperturbatively.

For the second Chern number of a reconstructed fiber bundle, eq. (5.5) implies

$$\chi_t^0 = \chi_t + C(a\Lambda)^{p_1} |\ln(a\Lambda)|^{p_2} + \cdots, \qquad (5.6)$$

where χ_t^0 is the bare susceptibility that emerges from the simulation, and χ_t is the physical susceptibility which we wish to extract.

The configurations responsible for $C \neq 0$ in eq. (5.6) are certain structures of size $\approx O(a)$ called *dislocations*.[44,45] A dislocation has three traits which imply that the fluctuations about them contribute to χ_t^0. A dislocation is 1) a quasistable (i.e. $\partial_t S = 0$) configuration with 2) action less than a instanton, and 3) its neighborhood contains configurations with $Q \neq 0$. Dislocations are qualitatively distinct from lattice instantons. The latter are more stable: both instantons and dislocations are saddle points, for generic lattice actions, but there is a narrower channel out of the instanton saddle point. Lattice instantons have action very close to the continuum value $4\pi^2\beta/N$; and they can have any size from a to $V^{1/4}$. To suppress dislocations one can alter the choice of Q, so that the boundary of the $Q \neq 0$ sector changes, or the choice of S, so that the action of the dislocation increases above $4\pi^2\beta/N$. The effect of this strategy is to reduce C and/or increase p_1 in eq. (5.6).

One estimates the exponents p_i in the following way. In the continuum limit the topological susceptibility in lattice units scales according to the asymptotic formula

$$\chi_t \propto \left[\frac{1}{a} \beta^{\beta_2/\beta_1^2} \exp\left(-\frac{\beta}{4N\beta_1} \right) \right]^4, \qquad (5.7)$$

where 4 is the dimension of spacetime, $\beta = 2N/g^2$, and $\beta_{1,2}$ are the first two coefficients of the perturbative Callan-Symanzik β-function:

$$\beta_1 = \frac{11N}{48\pi^2}, \quad \beta_2 = \frac{17N^2}{384\pi^4}. \qquad (5.8)$$

(Recall that the anomalous dimension vanishes.) The fluctuations about the dislocation provide a contribution to the bare susceptibility that scales as

$$\chi_t^{\text{dislocation}} \propto \frac{1}{a^4} \beta^{p_3} \exp(-\bar{S}_{\min}\beta), \qquad (5.9)$$

according to a semiclassical expansion[45] about the dislocation with minimum action $S_{\min} = \beta \bar{S}_{\min}$; $p_3 \neq 0$ accounts for entropy effects. The semiclassical expansion assumes a dilute gas of dislocations, and it should be reliable asymptotically. By folding eq. (5.7) and eq. (5.9) together, one obtains

$$p_1 = 4N\beta_1 \bar{S}_{\min} - 4 \qquad (5.10)$$

and

$$p_2 = 2(p_3 - \frac{2N\beta_2 \bar{S}_{\min}}{\beta_1}). \qquad (5.11)$$

Equations (5.10) and (5.11) assume that β is large enough so that perturbative two-loop scaling and the dilute gas of dislocations are valid approximations. In practice, this can only be determined *a posteriori* by doing a numerical simulation.

5.3. CP^{n-1} models in two dimensions

The CP^{n-1} models in two dimensions are asymptotically free, and they have a topological structure very similar to $SU(N)$ gauge theories in four dimensions. The fundamental variables of CP^{n-1} models are $n \times n$ complex projection matrices of rank 1:

$$P^2 = P, \quad P = P^*, \quad \mathrm{tr}P = 1. \tag{5.12}$$

As a warmup to the real problem, Berg and Lüscher[46] introduced a definition for CP^{n-1} lattice models with the same nice topological properties as those described in sec. 3. Of course, many details are drastically simpler. For the simplest model, CP^1 — equivalent to the $O(3)$ nonlinear σ model — the topological susceptibility χ_t did not exhibit any reasonable scaling behavior in a region where two other observables, the magnetic susceptibility and the correlation length, scaled universally.[46,47]

The CP^1 model, however, has the unhappy situation that $p_1 < 0$, so scaling χ_t should not be expected. In this case, Lüscher[45] computes $p_3 = -1$ and estimates $\bar{S}_{\min} \approx 6.69$. For CP^{n-1} models, asymptotic scaling reads

$$\chi_t \propto \left[\frac{1}{a}\beta^{2/n}\exp\left(-\frac{4\pi\beta}{n}\right)\right]^2, \tag{5.13}$$

whence $p_1 = 6.69n/4\pi - 2$, for $n = 2$ (i.e. CP^1) $p_1 = -0.935$. In fact, the Monte Carlo data reproduce the two-dimensional version of eq. (5.9) with $\bar{S}_{\min} \approx 6.69$ very well.

The CP^1 model was doomed to failure because it turns out that $\bar{S}_{\mathrm{instanton}} = 4\pi$, which coincides with the coefficient of β in the scaling law. Inasmuch as a lattice instanton always has an action slightly smaller than in the continuum (due to finite V and nonzero a effects), it is extraordinarily difficult to control dislocations. By modifying the lattice action one can raise $\bar{S}_{\min}$ to slightly less than 4π, but then the dislocations look just like small instantons. The only procedure that remains is to surgically remove the malignant dislocations,[48] but extending this to four dimensions is rather daunting. Moreover, the CP^1 model is a very exceptional case even in the continuum, where semiclassical instanton amplitudes have terrifying ultraviolet properties: in this model topology simply does not seem to make a lot of sense beyond classical field theory.

While refs. 46, 44, and 45 and the problems of the CP^1 model are well known, the really important work of Petcher and Lüscher[49] is usually overlooked. Any discussion of dislocations that omits this paper is incomplete and probably misleading. Reference 49 studies CP^{n-1} models for $n > 2$; unlike the $n = 2$ case the topological susceptibility is well behaved in the semiclassical expansion. For $n > 2$ one still has $\bar{S}_{\mathrm{instanton}} = 4\pi$ and $\bar{S}_{\min} \approx 6.69$ (embedded CP^1 instanton and dislocation), but now the asymptotic scaling coefficient is $2 \cdot 4\pi/n$. Already for $n = 3$ the coincidence of the instanton action and the β-function coefficient is lifted, and for $n > 4$ even the standard action supresses dislocations. Furthermore, ref. 49 shows that for an action improved to suppress small scale fluctuations, one can in practice obtain $\bar{S}_{\min} > 8\pi/3$ in the $n = 3$ model, and they observed universal scaling of χ_t with the correlation length ξ.

5.4. Determination of p_1 in $SU(N)$ gauge theory

To investigate the properties of dislocations in $SU(N)$ gauge theory in four dimensions we have turned to the mixed fundamental-adjoint action:

$$S = \sum_p \beta_f(1 - \frac{1}{2}\mathrm{tr}(U_p)) + \beta_{ad}(1 - \frac{1}{4}\mathrm{tr}^2(U_p)). \tag{5.14}$$

For $\beta_{ad} < 0$ (> 0) this action suppresses (enhances) dislocations (compared to the standard Wilson action $\beta_{ad} = 0$). Starting from a fixed $SU(2)$ configuration with $Q = 1$, we have searched for quasistable configurations using the diffusion equation on the group mani-

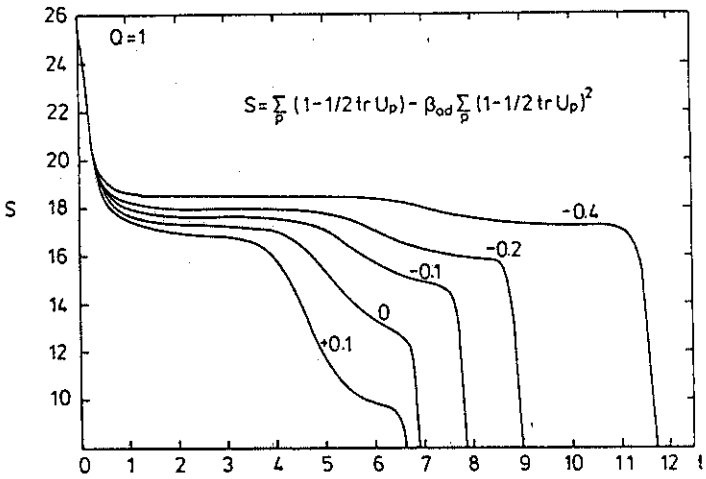

Figure 4: Cooling history of a smooth $Q = 1$ configuration. The value of the action S (defined in the figure) is plotted versus the time of diffusion. For $\beta_{ad} = +0.1$ the dislocation plateau is below the β-function value 10.77. All dislocations have Wilson action very close to $\bar{S} = 12$; after decay of the dislocation, the topological charge (using the Phillips-Stone algorithm) is $Q = 0$.

fold in the Euler approximation. Specifically, we replace iteratively the configuration $\{U_\ell\}$ by $\{U_\ell'\}$ obtained by

$$U_\ell' = \exp(-\varepsilon \partial_\ell S) U_\ell \qquad (5.15)$$

with stepsize $\varepsilon = 0.025$. In eq. (5.15) ∂_ℓ denotes group covariant differentiation with respect to the parallel transporter U_ℓ. The history of the "cooling" is shown in fig. 4 for five choices of couplings (β_f, β_{ad}) such that $\beta_f + 2\beta_{ad} = 1$, which ensures that all have the same naive continuum limit. On each curve one can perceive two plateaus: the first, especially stable one corresponds to the instanton; the second, less stable one is the dislocation. Using the topological charge program we have verified that $Q = 0$ after the collapse of the dislocation. From this plot one can read off the value of the action for the dislocation, as collected in Table 3. Notice that even the Wilson action has $\bar{S}_{\min} > 12\pi^2/11 = 10.77$. For $\beta_{ad} \geq -0.1$ the action profile of the dislocation obtained in this way resembles that of a fluxon: the six plaquettes surrounding a specific link have a high action

Table 3: Minimum action of the $Q = 1$ sector and fluxon action for various parameters in the adjoint action.

β_f	β_{ad}	$\bar{S}_{\min}$	$\bar{S}_{\text{fluxon}}$
0.8	+0.1	9.6	9.6
1.0	0.0	12.7	12.0
1.2	−0.1	14.7	14.4
1.4	−0.2	15.9	16.8
1.8	−0.4	17.2	21.6

density, whereas the rest of the plaquettes have negligible action density. The fluxon itself is the extreme case where the six plaquettes have $\text{tr}(U_p) = -2$; it is exceptional, but there are configurations in its neighborhood with $|Q| \neq 0$. For the $SU(N)$ Wilson action the fluxon has $\bar{S}_{\text{fluxon}} = 24/N$, so using it as a guide for $\bar{S}_{\min}$ one finds

$$p_1 = 4(\frac{11N}{2\pi^2} - 1), \qquad (5.16)$$

which yields $p_1 = 0.458$ for $SU(2)$ and $p_1 = 2.687$ for $SU(3)$.

Let us now return to the probability distribution P_Q. In this language the lesson of the foregoing analysis is that the continuum limit of the distribution is unaffected by dislocations if the exponent $p_1 > 0$. Dislocations still alter the charge assigned to a given configuration, but any systematic tendency to broaden the distribution disappears.

6. OTHER WAYS TO DEFINE Q

The formal part of the review is now finished, and it is time to confront the numerical work. First, this section discusses two other methods for identifying the topological charge of a lattice gauge field. The reader may wonder why one should bother to invent other methods. There are two reasons. One is that the fiber bundle methods were initially very slow: explicit interpolation consumes enormous amounts of CPU time. For $SU(2)$ this issue is entirely resolved with the Phillips

and Stone algorithm. The other is that there has been some skepticism that fiber bundle methods yield reliable values of χ_t. Either one feared a large value of C in eq. (5.6), so that contemporary simulations were in doubt, or one feared $p_1 < 0$ (as in the CP^1 model) so that the continuum limit was pathological. According to the analysis of the previous section, the second fear is unfounded, and in the next section the data indicate that C is small.

The two alternate methods are the "cooling" and "fermionic" methods. They both use physics rather than mathematics to interface the classical and semi-classical aspects of topology with the lattice.

6.1. Cooling

Cooling was first introduced for the CP^1 model,[44] in order to reconcile the classical topological structure with the unsatisfactory numerical results. The idea is to systematically lower the action in a way that uncovers quasistable configurations. One can either use the diffusion equation[50] as in sec. 5, or a "heat-bath" method, which replaces each link $U_{x,\mu}$ — in $SU(2)$ — by

$$U'_{x,\mu} = \frac{1}{M} \sum_{\nu \perp \mu} U_{x,\nu} U_{x+\nu,\mu} U_{x+\mu+\nu,-\nu}, \qquad (6.1)$$

where M ensures that the right-hand-side is in $SU(2)$. For the generalization to $SU(3)$ see, e.g., ref. 51.

This method is a very useful heuristic tool for understanding the structure of the QCD vacuum. For example, it has been used to motivate the choice of lattice action by insisting that the stability of the lattice instanton be increased,[52] or to construct configurations for which one can verify the index theorem.[53,54]

For large scale computations of the susceptibility,[15,17] the aim of the cooling method is to eliminate the dislocations. In the crudest method,[51] one cools equilibrium configurations and monitors the action until it becomes stable, and then the charge is deduced from the value of the action, via eq. (1.8). This charge is assumed to be the charge of the initial configuration. An improvement[15] cools for a small number of iterations, so that the charge is less likely to change, and the charge is determined by a simple approximant to the charge density such as in eq. (4.1). In addition to being a bit more reliable, this modification needs less computer time.

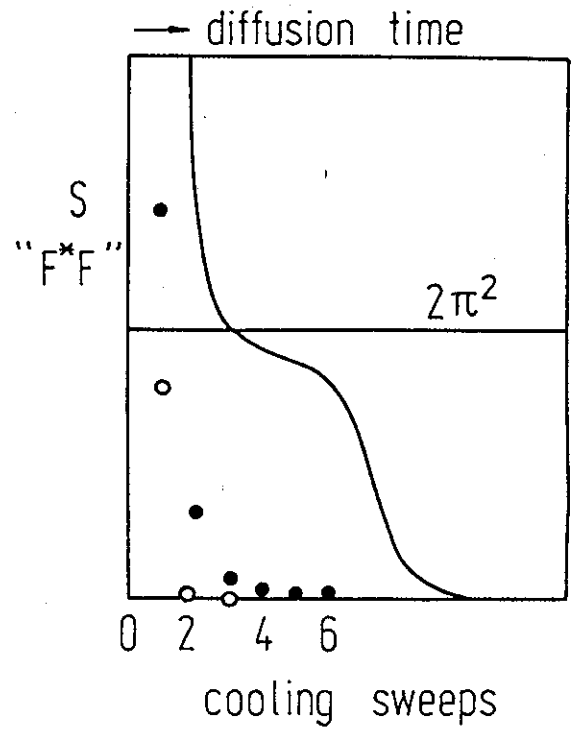

Figure 5: History of the configuration of ref. 55 during cooling. • shows the action and ○ the lattice approximant to the topological charge using the method of ref. 51, 15, and 17, in units so that both are $2\pi^2$ for an exact instanton. The solid line shows the fate of this configuration using diffusion.

If cooling eliminates dislocations it obviously eliminates small instantons as well. This leads to a systematic error which is very hard to quantify. Even more striking, the cooling algorithm defined by eq. (6.1), which is used in refs. 51, 15, and 17, can even miss large instantons. In fig. 5 we show the evolution of the action and those references' lattice approximant to $\int d^4x \ \mathrm{tr}\{F_{\mu\nu}{}^*F_{\mu\nu}\}$ during cooling. The starting configuration is the lattice instanton of ref. 55 with core diameter $6a$ on a 12^4 lattice. By construction it has $Q = 1$, and in practice both the algorithms of Lüscher and of Phillips and Stone yield $Q = 1$. Also, the stag-

gered fermion matrix has a zero mode.[55] In summary, the configuration has the topological and physical structure of a semiclassical instanton surrounded by quantum fluctuations. Under the cooling algorithm of refs. 51, 15 and 17 it just dies. Curiously, the diffusion equation preserves the instanton (now with core diameter $3a$ on a 6^4 lattice, which might be *less* stable), presumably because it is based on the equations of motion, and hence it cools more slowly.

The net effect of these systematic effects is that the distribution obtained by the cooling method is too narrow, and the $\langle Q^n \rangle_c / V$ derived from it are severe underestimates.

6.2. "Fermionic" methods

In QCD the topological charge is related to the axial current through the anomaly, eq. (2.1). The "fermionic" proposal is to use this relationship to construct a definition of the lattice topological charge.[56] This has several advantages and disadvantages, which will simply be listed here. I will not go into details, because Vink's contribution[29] represents the state of the art, and that is not yet well enough developed to be included in the next section's numerical summary.

The main advantage is that it connects to the Atiyah-Singer index theorem and the physics it implies. Configurations with nonvanishing Q have zero modes, and hence they are suppressed by $\det(\not{D} + m) \approx 0$. The fermionic method is designed to reproduce this magic on the lattice, albeit with an approximate Dirac operator that does not satisfy the theorem. This is nice, but for investigating the Witten-Veneziano formula it is not especially compelling, because the *pure glue* susceptibility enters. Very compelling is the new derivation of the Witten-Veneziano formula,[28] in which the susceptibility of the Atiyah-Singer index enters naturally, rather than the topological susceptibility.

A neutral observation questions the point of bringing fermions an arena which also concerns itself with the *construction* of quantized gauge fields.

In theory the fermions may incorporate the right physics, but in practice they also obscure it. The lattice regulator invariably breaks the $U_A(1)$ symmetry explicitly, otherwise it would be impossible to get the anomaly right. Consequently, fermionic definitions are based on operators that do not have the special properties needed to avoid $\kappa_\chi \neq 1$, and the reliable determination of κ_χ seems difficult.[29] Furthermore, the notorious numerical problems of fermions also raise their ugly head.

7. NUMERICAL ASPECTS AND RESULTS

Now that the mathematics and physics are clear, it is time to apply the algorithms of the previous sections to a Monte Carlo simulation. This will be done first for $SU(2)$ and then for $SU(3)$, and in each case the fiber bundle and cooling methods are compared. Since the analysis of sec. 5.4 indicates that dislocations are not a problem, this section tacitly assumes $\chi_t = \chi_t^0$. Similarly, systematic effects in the cooling method — lost instantons and/or $\kappa_\chi \neq 1$ — will be ignored. Finally, there will be some general remarks tying into the Witten-Veneziano formula.

7.1. Results in SU(2)

Figure 6 shows Monte Carlo results for $a^4\chi_t$ in $SU(2)$ obtained by two fiber bundle methods[16,10,11] and by the improved cooling method[15] on L^4 lattices of various sizes. Except for the $*$'s and the $\blacktriangle$'s all simulations were done with the Wilson action. The solid line represents the $\beta = 2.6$, $L = 12$ result extended to other values of β using the two-loop scaling formula, eq. (5.7). Reference 16 (the $\blacksquare$'s) uses Woit's[7] algorithm and refs. 10 and 11 (the $\bullet$'s, $*$'s, and $\blacktriangle$'s) use Phillips' and Stone's algorithm[8] on a hypercubic lattice sliced into simplices.[10] Within errors the two calculations using a direct determination of the charge agree. (The errors for the $\bullet$'s are too small to plot in fig. 6; some of the error bars from the $\blacksquare$'s run into the $\bullet$'s.) In the simulations for which the author (as opposed to his collaborators) has personally collected the statistics, he has noticed that the central value of the susceptibility *increases* slightly as statistics are increased from that of

the ■'s to that of the •'s. If this experience were to apply to ref. 16 also, then the agreement might even improve. The discrepancy between the topological methods and the cooling method is due mostly to instantons annihilated by cooling and, at smaller values of β, perhaps to the dislocations as well.

To investigate the dislocation contribution fig. 6 also shows values of the susceptibility obtained using the mixed fundamental-adjoint action, eq. (5.14). They are plotted against $\beta = 4/g^2$ obtained using the one-loop expression[57]

$$\beta = \beta_f + 2\beta_{ad} - \frac{5}{2}\frac{\beta_{ad}}{\beta_f + 2\beta_{ad}} \qquad (7.1)$$

which is consistent with the scaling behavior in previous work,[58,59] as long as the one-loop term remains small. The three $*$'s have $(\beta_f, \beta_{ad}) = (2.3, 0.1)$, $(2.3, 0.2)$, and $(2.3, 0.3)$ which enhance dislocations by decreasing p_1 in eq. (5.6). The dashed line through them indicates dislocation dominated scaling with $\bar{S}_{\min} = 9$, which is the $\bar{S}_{\min}$ for $(\beta_f, \beta_{ad}) = (2.3, 0.2)$. The two ▲'s have $(\beta_f, \beta_{ad}) = (2.7, -0.2)$ and $(3.0, -0.5)$ which suppress dislocations by increasing p_1. They agree with the Wilson action results within statistical errors in χ_t and systematic errors in β.

Reference 11 has extended the work of ref. 10 to the point where the errors are so small that one can begin to disentangle scaling violations from finite volume effects. Ideally one would like to compare a dimensionless measure of the physical volume, such as $z_\lambda \equiv La\chi_t^{1/4}$, to another dimensionless ratio of physical observables. Figure 7 uses the two-loop Λ_L parameter because the scaling behavior of fig. 6 is so tantalizing, and in order to avoid the statistical error of another numerical simulation. If the nonuniversal terms in eq. (5.6) are negligible, and if two-loop scaling applies, the Monte Carlo data should lie on a smooth curve. For $\beta \geq 2.5$ the data do indeed lie on the dashed curve, drawn to guide the eye. In similar plots with other coefficients of β in the scaling law, for instance $\bar{S}_{\min}$, the Monte Carlo data at different β values do not lie on a univer-

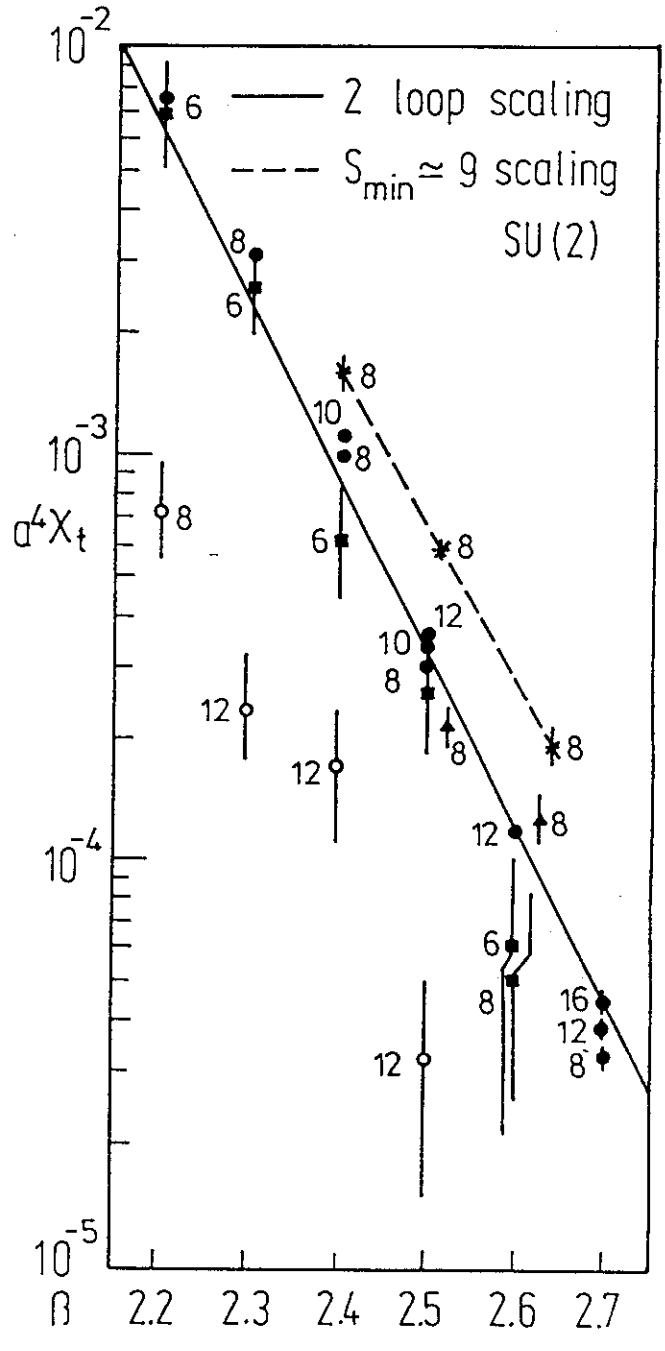

Figure 6: Topological susceptibility in $SU(2)$ lattice gauge theory. The number next to the symbols are the lattice size L. • uses Phillips' and Stone's charge, refs. 10, 11; for these points the errors are too small to plot. $*$ uses Phillips' and Stone's charge and an adjoint action that *favors* dislocations. ▲ uses Phillips' and Stone's charge and an adjoint action that *suppresses* dislocations. ■ uses Woit's charge, ref. 16. ○ uses heat-bath cooling and q_{naive}, ref. 15.

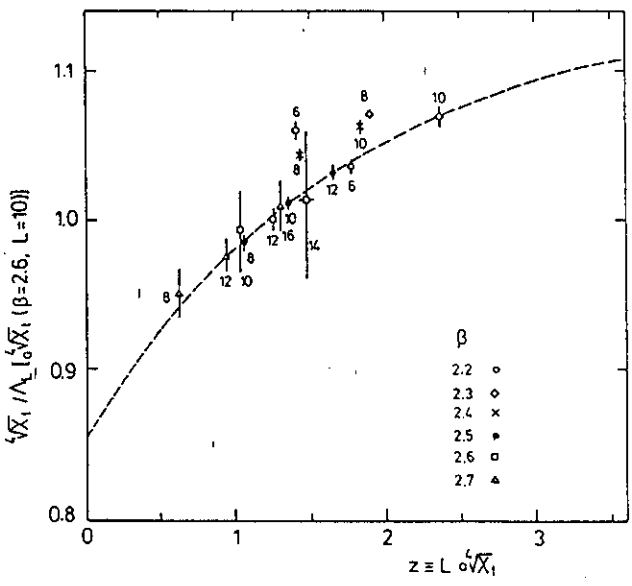

Figure 7: $\chi_t^{1/4}/\Lambda_L$ – in units of the value from the $\beta = 2.6$, $L = 12$ simulation – vs. $z \equiv La\chi_t^{1/4}$ (z is called z_χ in the text.) The dashed line emphasizes that the data for $\beta \geq 2.5$ lie on a universal curve.

sal curve on the scale of the fine vertical axis of fig. 7. This indicates that the constant C in eq. (5.6) does not dominate the bare susceptibility.

Now consider the data for $\beta < 2.5$. It is known from other numerical simulations[60] that $\Delta\beta(\beta)$, the shift in β needed to produce a factor-of-two scale change, has a dip centered at $\beta \approx 2.3$ This means that the lattice spacing a in the range $2.2 < \beta < 2.5$ is larger than that given by the two-loop formula. Had fig. 7 taken this phenomenon into account, the Monte Carlo data at $\beta = 2.3$ and 2.4 would lie upon a single curve with the data at other values of β. Moreover, bringing all the data onto a universal curve, yields a result consistent with an approach to infinite volume exponential in $z' = 4.7z_\chi$. Comparing the topological susceptibility to the mass gap calculations[61] one also finds $z_{\text{mass gap}} \equiv Lam \approx 4.7z_\chi$.

7.2. Results in SU(3)

Figure 8 shows Monte Carlo results for $a^4\chi_t$ in $SU(3)$ obtained by two fiber bundle methods[18,19] and by the improved cooling method[17] on L^4 lattices of various sizes. Reference 19 (the •'s) uses the section[14] for Lüscher's bundle,[5] whereas ref. 18 (the ■'s) uses Woit's algorithm.[7] As in $SU(2)$ the two fiber bundle methods agree, within errors, but the cooling method gives values which are rather smaller, although the disparity is less marked than in $SU(2)$. The apparent agreement between refs. 17 and 19 at $\beta = 6.0$ may be illusory, because the volumes are quite different, and one expects the susceptibility to increase monotonically. The disagreement at $\beta = 5.85$ is probably more indicative of the situation, because there both simulations are at $L = 8$.

At larger values of β both methods yield results that scale with the string tension measurements of ref. 62; the solid line is drawn through the $L = 10$, $\beta = 6.0$ point and scales as K^2. For the fiber bundle results, this means that the estimate of p_1 in sec. 5 is a bit high for $SU(3)$, although it still remains positive. Note that although the susceptibility and the string tension seem to scale universally, the scaling is very different from two-loop scaling (dashed line).

7.3. General remarks

Table 4 list the results for the topological susceptibility for both $SU(2)$ and $SU(3)$, using the string tension or ρ meson mass to set the physical scale. The numbers are to be compared to the "prediction" of $(180\text{MeV})^4$ from eq. (2.5). The result of the cooling method in $SU(3)$ agrees best with the prediction, but one should keep the unknown accuracy of the assumption $f_{\eta'} = f_\pi$ in mind. In fact, since dislocations seem *not* to be a problem, perhaps one should use the fiber bundle results to predict $f_{\eta'}/f_\pi$.

It is intriguing that the fiber bundle and cooling methods show the same scaling behavior in both groups, even though the latter purges small instantons and annihilates the occasional large instanton as well, cf. fig. 5. Evidently the cooling method still includes fluctuations from enough length scales, so that the $\exp(-\beta/4N\beta_1)$ renormalization group behavior can build up from the semiclassical $\exp(-4|Q|\pi^2\beta/N)$ instanton behavior.

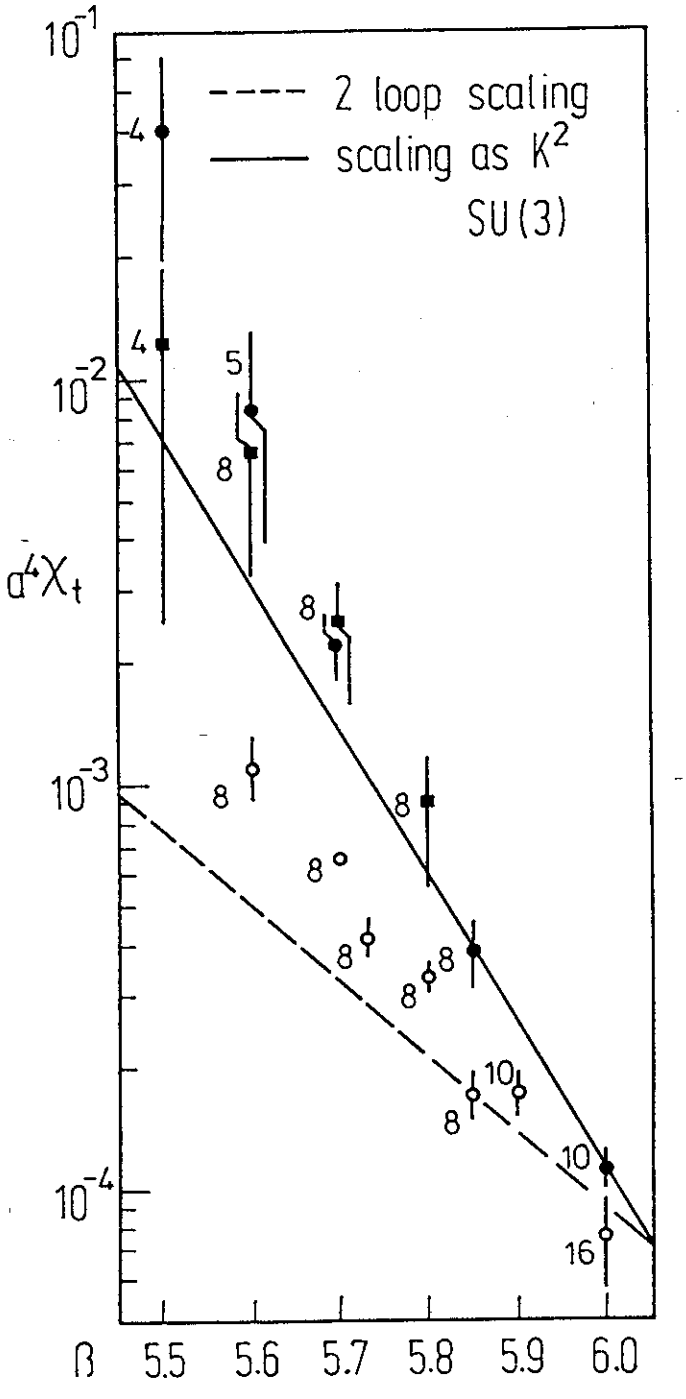

Figure 8: Topological susceptibility in $SU(3)$ lattice gauge theory. Again, the number next to the symbols are the lattice size L. • uses Lüscher's charge, refs. 19. ■ uses Woit's charge, ref. 18. ○ uses heat-bath cooling and q_{naive}, ref. 17.

Table 4: Compendium of values of χ_t. Errors are statistical only.

group	**method**	β	L	χ_t
$SU(2)$	Ph-S	2.4	8,10	$(262 \pm 1$ MeV$)^4$
$SU(3)$	Lüscher	6.0	10	$(231 \pm 10$ MeV$)^4$
$SU(2)$	cooling	2.4	10	$(130 \pm 10$ MeV$)^4$
$SU(3)$	cooling	5.9	10	$(190 \pm 7$ MeV$)^4$

Unfortunately, the $SU(3)$ charge consumes too much computer time to attain the precision of ref. 11. This problem will remain until we have a suitable algorithm. The Phillips and Stone bundle in $SU(3)$ has all the nice properties of the $SU(2)$ bundle, except that the homotopy classes of the section cannot be worked out combinatorically. Can this be achieved, using reduction, perhaps? The interested reader is encouraged to find out.

8. CONCLUDING REMARKS

The beginning of this review argued that it is important to seek and understand the meaning of lattice gauge fields; let us recall why. Topologically nontrivial configurations play an intrinsically nonperturbative role. Consequently there ought to be room for them within the framework of the nonperturbative regulator. Moreover, semiclassical considerations imply that these configurations are crucial for understanding the pseudoscalar meson masses, the masses which in fact require chromodynamics and not just the quark model. Hence, it seems unwise to throw out the concept of topology simply for the sake of the CRAY 2 or the ETA 10.

Naively a lattice field has no topology, "because any lattice field can be deformed into any other." However, mathematicians can talk about the topology of the integers, a space with little room for continuous deformation as defined by common usage. In the case of gauge fields the topology is entirely contained in the coordinate bundle, i.e. the set of transition functions. One can

define transition functions for lattice gauge fields,[5] and for sufficiently smooth configurations the bundle so defined not only exists, but also is unique.[8] The space of all lattice gauge fields are split into sectors, separated by exceptional configurations for which the charge is mathematically not defined. It is only possible to continuously deform from one sector to another by passing through an exceptional configuration.

The topology of the reconstructed bundle is also the correct topology for QCD, for two reasons. First of all, the second Chern number of the lattice gauge field is the "topological charge," if the field is smooth. There are two ways to see this. One can derive the expression for the Chern-Pontryagin density and check that it reduces to $-\mathrm{tr}\{F_{\mu\nu}{}^*F_{\mu\nu}\}/16\pi^2$ in the continuum limit. Alternatively, one can use the uniqueness theorem[8] for smooth fields: all lattice gauge fields close enough to a given continuum gauge field give the same topological charge.[63] Secondly, asymptotic freedom ensures that smooth fields dominate the path integral, at least with sensible regularization, so that the (quantum) continuum limit of observables like the topological susceptibility can be determined.

With a solid formal ground to stand on, one can now compute the topological susceptibility. The results summarized in Table 4 demonstrate that the Witten-Veneziano explanation of the $U_A(1)$ problem is correct; topology accounts for the mass of the η' (and perhaps its decay constant?) in a quantitative way. This conclusion also stands if one prefers other approaches to the topological susceptibility, such as the cooling method.

The topological susceptibility χ_t is also an ideal tool for studying the various features of numerical simulation. It is an observable quantity that suffers no (multiplicative) renormalization, yet it is not the result of a fit, like the string tension or the mass gap. Hence χ_t is easy to compute, and with enough precise simulation data one can disentangle finite volume and nonzero lattice spacing effects from true scaling behavior.[11] Given the bleak forecast for determining the heavy quark potential at long distances,[64] this is significant. Unfortunately, χ_t cannot be measured by experimentalists, so it cannot be used to set the physical scale. Also, the lack of combinatoric methods for $SU(3)$ constitute a major barrier to high statistics simulations with the physical gauge group.

For $SU(2)$ all of the technological barriers have been tackled. The charge algorithm is fast and easily vectorizable: Q_α can be computed for many cells in parallel. This has enabled us to obtain very precise Monte Carlo data.[11] The z-plot, fig. 7 is consistent with asymptotic scaling for $\beta \geq 2.5$, and indicates that the susceptibility is suppressed at small volumes and nonzero temperature, as first seen with the cooling method.[17] The suppression sets in near $z_\chi \sim 1$, which corresponds to $z_{\text{mass gap}} \sim$ 4.5-5.0, which concurs with expectations from analytic calculations in a finite volume.[65]

The data is also precise enough that we can make an honest attempt at studying the θ-vacuum.[66]

There are several interesting topological aspects of lattice gauge theories that I have ignored in this review, in order to have a sharp focus and to stay within the page and time limits. The role of color magnetic monopoles in the deconfinement transition is an old problem.[67,68] These monopoles are dynamical variables in a certain gauge[69] with a residual $U(1)^{N-1}$ gauge group. The necessary abelian projection can be formulated on the lattice,[70] and numerical results show that the monopoles behave rather differently in the two phases.[71] Furthermore, the monopoles are just one example of solitons, which can indeed be quantized using the lattice.[72]

Let me end with a possibly crazy suggestion. At several points I have pointed out that neither the Dirac operator of Wilson nor of staggered fermions has topological significance. Given the numerical and conceptual problems of lattice fermions and the physical appeal of the index theorem, one cannot help but wonder if topology could be the missing guide to a more satisfactory

formulation. One can, for example, reconstruct associated bundles for matter fields,[73] put the fermions on a finer lattice[28], or keep them in the continuum.[74] All of these ideas are too impractical, but maybe they are on the right track.

ACKNOWLEDGEMENTS

Doug Photiadis once said, "You should look into topology sometime, if you get around to it, Andreas!" Since "getting around to it" I have benefited from conversation, collaboration, and consultation with I. Barbour, B. Berg, M. Göckeler, R. Horgan, H. Joos, M. Kremer, M.L. Laursen, M. Lüscher, M. Marcu, M. Müller-Preußker, A. Phillips, J. Polonyi, G. Schierholz, C. Schleiermacher, F. Wagner, U.-J. Wiese, and U. Wolff on topological aspects of lattice gauge theories. Finally, I would like to thank the organizing committee for inviting me to review this subject, and my fellow conference participants for discussion and, in some cases, debate. In particular, thanks to P. van Baal for a beer and to P. Rossi for several Toscani cigars.

REFERENCES

1. Reprints of early work have been collected by C. Rebbi, *Lattice Gauge Theories and Monte Carlo Simulations* (World Scientific, Singapore, 1983). The present volume is (by definition) the most recent snapshot of new progress.
2. E. Seiler, *Gauge Theories as a Problem of Constructive Quantum Field Theory and Statistical Mechanics* (Springer-Verlag, Berlin, 1982).
3. M.E. Peskin, Cornell University Ph.D. thesis and report CLNS-395 (1978).
4. P. di Vecchia, K. Fabricius, G.C. Rossi, and G. Veneziano, *Nucl. Phys.* **B192** (1981) 392; *Phys. Lett.* **108B** (1982) 323.
5. M. Lüscher, *Commun. Math. Phys.* **85** (1982) 29.
6. P. Woit, *Phys. Rev. Lett.* **51** (1983) 638.
7. P. Woit, *Nucl. Phys.* **B262** (1985) 284.
8. A. Phillips and D. Stone, *Commun. Math. Phys.* **103** (1986) 599;
   G. Lasher, A. Phillips, and D. Stone, in *Quark Confinement and Liberation: Numerical Results and Theory*, edited by F. Klinkhammer and M.B. Halpern (World Scientific, Singapore, 1985).
9. M.L. Laursen, G. Schierholz, and U.-J. Wiese, *Commun. Math. Phys.* **103** (1986) 693;
   M. Göckeler, M.L. Laursen, G. Schierholz, and U.-J. Wiese, *Commun. Math. Phys.* **107** (1986) 467.
10. A.S. Kronfeld, M.L. Laursen, G. Schierholz, and U.-J. Wiese, *Nucl. Phys.* **B292** (1987) 330.
11. M. Kremer, A.S. Kronfeld, M.L. Laursen, G. Schierholz, C. Schleiermacher, and U.-J. Wiese, DESY report in preparation.
12. M. Atiyah and I.M. Singer, *Ann. Math.* **93** (1971) 139.
13. S. Weinberg, *Phys. Rev.* **D11** (1975) 3583.
14. U.-J. Wiese, *Topologie von (Gitter-) Eichfeldern*, Universität Hannover thesis (1986) in German.
15. M. Teper, *Phys. Lett.* **162B** (1985) 357; **171B** (1986) 81, 86.
16. Y. Arian and P. Woit, *Nucl. Phys.* **B268** (1986) 521.
17. J. Hoek, M. Teper, and J. Waterhouse, *Phys. Lett.* **180B** (1986) 112; *Nucl. Phys.* **B288** (1987) 589.
18. Y. Arian and P. Woit, *Phys. Lett.* **183B** (1987) 341.
19. M. Göckeler, A.S. Kronfeld, M.L. Laursen, G. Schierholz, and U.-J. Wiese, *Nucl. Phys.* **B292** (1987) 349; work in progress.
20. A.A. Belavin, A.M. Polyakov, A.S. Schwartz, and Y.S. Tyupkin, *Phys. Lett.* **59B** (1975) 85.
21. C.G. Callan, R.F. Dashen, and D.J. Gross, *Phys. Lett.* **63B** (1976) 334;
   R. Jackiw and C. Rebbi, *Phys. Rev. Lett.* **37** (1976) 172.
22. R.D. Peccei and H.R. Quinn, *Phys. Rev. Lett.* **38** (1976) 1440;
   for a recent review see the Erice lectures by W. Buchmüller, DESY report DESY 86/156.
23. S. Itoh, Y. Iwasaki, and T. Yoshié, *Phys. Lett.* **184B** (1987) 375; *Phys. Rev.* **D36** (1987) 527.
24. S. Adler, *Phys. Rev.* **117** (1969) 47;
   J.S. Bell and R. Jackiw, *Nuov. Cim.* **60A** (1969) 529.
25. E. Witten, *Nucl. Phys.* **B156** (1979) 269;
   G. Veneziano, *Nucl. Phys.* **B159** (1979) 213.
26. G. 't Hooft, *Phys. Rev. Lett.* **37** (1976) 8; *Phys. Rev.* **D14** (1976) 3432.

27. See M.E. Peskin, *Recent Developments in Field Theory and Statistical Mechanics*, 1982 Les Houches lectures, edited by J.B. Zuber and R. Stora (North-Holland, Amsterdam, 1984) for a review.

28. J. Smit and J. Vink, *Nucl. Phys.* **B284** (1987) 234; in *Lattice Gauge Theory 1986*, edited by H. Satz, I. Harrity, and J. Potvin (Plenum, New York, 1987); *Phys. Lett.* **194B** (1987) 433; Amsterdam preprint IFTA-87-7 (August 1987).

29. J. Vink, "Topological Charge, Zero Modes, and Restoration of Flavor Symmetry with Staggered Fermions," this volume.

30. M. Daniel and C.M. Viallet, *Rev. Mod. Phys.* **52** (1980) 175.

31. K. Ishikawa, G. Schierholz, H. Schneider, and M. Teper, *Phys. Lett.* **128B** (1983) 309.

32. N.V. Makhaldiani and M. Müller-Preußker, *JETP Lett.* **37** (1983) 523.

33. The following analysis has been stolen from ref. 10, which stole it from ref. 9.

34. P. van Baal, *Commun. Math. Phys.* **85** (1982) 529.

35. See C. Panagiotakopoulos, *Phys. Rev.* **D32** (1985) 1048 for a critique of ref. 6.

36. See A. Phillips, *Ann. Phys.* **161** (1985) 399 for the simpler version of this algorithm for $U(1)$ theory in 2 dimensions.

37. I.A. Fox, J.P. Gilchrist, M.L. Laursen, and G. Schierholz, *Phys. Rev. Lett.* **54** (1985) 749.

38. G. Parisi and F. Rapuano, *Phys. Lett.* **152B** (1985) 218.

39. A.S. Kronfeld and D.M. Photiadis, *Phys. Rev.* **D31** (1985) 2939.

40. G. Martinelli and Zhang Y.-L., *Phys. Lett.* **123B** (1983) 433; **125B** (1983) 77.

41. D.G. Richards, C.T. Sachrajda, and C.J. Scott, *Nucl. Phys.* **B286** (1987) 683.

42. L. Maiani, G. Martinelli, G.C. Rossi, and M. Testa, *Nucl. Phys.* **B289** (1987) 505.

43. C. Bernard, A. Soni, and T. Draper, UCLA report UCLA/87/TEP/18.

44. B. Berg, *Phys. Lett.* **104B** (1981) 475.

45. M. Lüscher, *Nucl. Phys.* **B200** (1982) 61.

46. B. Berg and M. Lüscher, *Nucl. Phys.* **B190** (1981) 412.

47. G. Martinelli, R. Petronzio, and M.A. Virasoro, *Nucl. Phys.* **B205** (1982) 255.

48. B. Berg and C. Panagiotakopolous, *Nucl. Phys.* **B251** (1985) 353.

49. D. Petcher and M. Lüscher, *Nucl. Phys.* **B225** (1983) 53.

50. M. Müller-Preußker, private communication.

51. J. Hoek, *Comput. Phys. Commun.* **39** (1986) 21; *Phys. Lett.* **166B** (1986) 199.

52. Y. Iwasaki and T Yoshié, *Phys. Lett.* **131B** (1983) 159.

53. E.-M. Ilgenfritz, M.L. Laursen, M. Müller-Preußker, G. Schierholz, and H. Schiller, *Nucl. Phys.* **B268** (1986) 693.

54. I. Barbour and M. Teper, *Phys. Lett.* **175B** (1987) 445.

55. I.A. Fox, M.L. Laursen, G. Schierholz, J.P. Gilchrist, and M. Göckeler, *Phys. Lett.* **158B** (1985) 332.

56. E. Seiler and I.O. Stamatescu, *Phys. Rev.* **D25** (1982) 2177; **D26** 534;
F. Karsch, E. Seiler, and I.O. Stamatescu, *Nucl. Phys.* **B271** (1986) 349.

57. A. di Giacomo and G. Paffuti, *Nucl. Phys.* **B205** (1982) 313.

58. G. Bhanot and M. Creutz, *Phys. Rev.* **D24** (1981) 3212.

59. G. Bhanot and N. Seiberg, *Phys. Rev.* **D29** (1984) 2420.

60. A. Patel and R. Gupta in *Advances in Lattice Gauge Theory*, edited by D.W. Duke and J.F. Owens (World Scientific, Singapore, 1985) and references therein.

61. B. Berg, A. Billoire, and C. Vohwinkel, *Phys. Rev. Lett.* **57** (1986) 400;
B. Berg in *Lattice Gauge Theory 1986*, edited by H. Satz, I. Harrity, and J. Potvin (Plenum, New York, 1987).

62. Ph. de Forcrand, G. Schierholz, H. Schneider, and M. Teper, *Phys. Lett.* **160B** (1985) 137.

63. Indeed, one of the motivations of ref. 8 was to find combinatoric methods for computing characteristic classes.

64. F. Gutbrod, "Do Creutz Ratios Scale Properly in $SU(2)$ Lattice Gauge Theory?" this volume; *Z. Phys.* **C** (in print).

65. P. van Baal, "Confronting Analytic and Monte Carlo Results in a Finite Volume for Pure Gauge Theories," this volume;
P. van Baal and J. Koller, *Ann. Phys.* **174** (1987) 299.

66. A.S. Kronfeld, M.L. Laursen, G. Schierholz, C. Schleiermacher, and U.-J. Wiese, DESY report in preparation.

67. D.J. Gross, R.D. Pisarski, and L.G. Yaffe, *Rev. Mod. Phys.* **53** (1981) 43.

68. J. Polonyi in *Lattice Gauge Theory 1986*, edited by H. Satz, I. Harrity, and J. Potvin (Plenum, New York, 1987).

69. G. 't Hooft, *Nucl. Phys.* **B190** (1981) 455.

70. A.S. Kronfeld, G. Schierholz, and U.-J. Wiese, *Nucl. Phys.* **B293** (1987) 461.

71. A.S. Kronfeld, M.L. Laursen, G. Schierholz, and U.-J. Wiese, *Phys. Lett.* **B** (in print);
U.-J. Wiese, "Confinement and the Dynamics of Magnetic Monopoles," this volume.

72. J. Fröhlich and P.A. Marchetti, *Commun. Math. Phys.* **112** (1987) 343.

73. M. Göckeler, A.S. Kronfeld, and U.-J. Wiese (unpublished).

74. R. Flume and D. Wyler, *Phys. Lett.* **108B** (1987) 317.